Title

Macromolecular fraction (MMF) from 3D ultrashort echo time cones magnetization transfer (3D UTE-Cones-MT) imaging predicts meniscal degeneration and knee osteoarthritis

Journal

Osteoarthritis and Cartilage, 29(8)

ISSN

1063-4584

Authors

Zhang, X
Ma, Y-J
Wei, Z
et al.

Publication Date

2021-08-01

DOI

10.1016/j.joca.2021.04.004

Peer reviewed

HHS Public Access

Author manuscript

Osteoarthritis Cartilage. Author manuscript; available in PMC 2022 April 01.

Published in final edited form as:

Osteoarthritis Cartilage. 2021 August ; 29(8): 1173–1180. doi:10.1016/j.joca.2021.04.004.

Macromolecular fraction (MMF) from 3D ultrashort echo time Cones magnetization transfer (3D UTE-Cones-MT) imaging predicts meniscal degeneration and knee osteoarthritis

Xiaodong Zhang, MD[1,2,+], **Ya-Jun Ma, PhD**[1,+], **Mei Wu, MD**[1], **Zhao Wei, MS**[1], **Aria Ashir, MD**[1], **Saeed Jerban, PhD**[1], **Eric Y Chang, MD**[3,1], **Shaolin Li, MD**[4], **Jiang Du, PhD**[1]

[1]University of California San Diego, San Diego, CA, United States

[2]Department of Radiology, The Third Affiliated Hospital of Southern Medical University, China

[3]Veterans Affairs San Diego Healthcare System, San Diego, CA, United States

[4]Department of Radiology, The Fifth Affiliated Hospital of Sun Yet-sen University, Zhuhai, China

Abstract

Objective: Meniscal degeneration is strongly associated with osteoarthritis (OA), but conventional sequences have limited values in the evaluation of meniscus due to its short T2 relaxation time. We aimed to evaluate a 3D ultrashort-echo-time Cones magnetization transfer (UTE-Cones-MT) sequence for quantification of macromolecular fraction (MMF) and MT ratio (MTR) in menisci of healthy volunteers and patients with different degrees of OA.

Methods: Patients with mild OA (n=19; 37-86 years; 10 males) or advanced OA (n=12; 52-88 years; 4 males) and healthy volunteers (n=17; 20-49 years; 7 males) were scanned with T2-FSE and 3D UTE-Cones-MT sequences on a 3T scanner. Morphological assessment was performed using meniscal whole-organ magnetic resonance imaging score (WORMS). MMF and MTR were calculated for anterior and posterior horns of medial and lateral menisci, and were correlated with age and meniscal WORMS scores of the three groups of human subjects. The diagnosis efficiency of MMF and MTR was performed by using receiver operating characteristic (ROC) curve and the area under the curve (AUC) analyses.

Results: Decreased MMF and MTR were observed in menisci of patients with mild or advanced OA compared with healthy subjects, and in menisci with tears (Grade 2-4) compared with normal menisci (Grade 0). Significant negative correlations were observed between MMF ($r=-0.769$, $P<0.01$), MTR ($r=-0.320$, $P<0.01$), and meniscal WORMS score. There was a mild negative correlation between MMF ($r=-0.438$, $P<0.01$), MTR ($r=-0.289$, $P<0.01$), and age. The AUC

Corresponding Author: Jiang Du, Ph.D., jiangdu@ucsd.edu, University of California San Diego, Department of Radiology, 9452 Medical Center Drive, La Jolla, CA 92037, United States, Phone: 858-246-2248.

[+]The authors contributed equally to this work.

Author Contributions

Xiaodong Zhang, Ya-jun Ma, Shaolin Li, Eric Chang and Jiang Du contributed to the concept and design of the study and the analysis and interpretation of the data. Ya-jun Ma and Saeed Jerban contributed to the acquisition of the data. Xiaodong Zhang, Ya-jun Ma, Zhao Wei , Mei Wu and Aria Ashir contributed to the analysis of data. Jiang Du and Eric Chang contributed funding for the study. All authors contributed to the drafting of the article and final approval of the version to be submitted.

Conflict of interest

There are no conflicts of interest in this paper.

values of MMF and MTR in the four horns of meniscus and the posterior horn medial meniscus for differentiating OA patients from healthy volunteers were 0.762 and 0.699, and 0.835 and 0.883, respectively.

Conclusion: The 3D UTE-Cones-MT biomarkers of MTR and especially MMF can detect compositional changes in meniscus and differentiate healthy subjects from patients with mild or advanced knee OA.

Keywords

Ultrashort echo time(UTE); Magnetization Transfer(MT); meniscus; osteoarthritis; Quantitative; Diagnosis

Introduction

The menisci play a vital protective role in the long-term health of the knee joint by facilitating shock absorption and load distribution. Meniscal degeneration is known to be strongly associated with the development and progression of osteoarthritis (OA) (1–2). Early detection of compositional changes in the meniscus is of critical importance in preserving the tissue and avoiding the onset or progression of OA. Various quantitative magnetic resonance imaging sequences have been used to evaluate biochemical changes in meniscal tissues (3–5). These techniques such as T1ρ and T2 are potentially more sensitive than conventional morphological sequences in identifying early signs of meniscal deterioration (3–7). However, both conventional T1ρ and T2 are affected by the magic angle effect (5,8). A previous study of articular cartilage indicated that changes in conventional T1ρ and T2 values due to the magic angle effect can be more than those caused by degeneration (9). This is likely to affect their performance in evaluating meniscal degeneration and early diagnosis of OA.

Magnetization transfer (MT) imaging has also been used for indirect assessment of macromolecules in biological tissue (10,11) to explore its value in the early diagnosis of OA. The simplest approach is to measure the magnetization transfer ratio (MTR), which provides a measure of the magnetization change before and after the MT pulse. Reduction in MTR has been shown to be associated with collagen degradation and proteoglycan depletion (11–13). However, the functional use of cartilage MTR values is limited (12). In regards to meniscus, MT imaging has been less studied since meniscal MTR and MT modeling are challenging (14). The fundamental technical challenge is related to the meniscal structure. The meniscus is a collagen-rich tissue consisting of highly organized distinct groups of collagen fibers, including the meshwork fibers covering the meniscus surfaces, the lamella-like collagen fibril bundles beneath the superficial network, the radial fibers located in the external circumference of the anterior and posterior segments, and the main circumferential fibers located in the central region between the femoral and tibial surface layers (15). This highly organized fiber structure leads to a strong dipole-dipole interaction and, subsequently, a short T2 relaxation (16). As a result, the meniscus typically shows as little or low signal when imaged with conventional clinical sequences (17).

In comparison, ultrashort echo time (UTE) sequences with TEs ~100 times shorter than those of conventional sequences allow direct imaging of short T2 tissues such as the meniscus (17). More recently, a three-dimensional multi-spoke UTE Cones MT sequence (3D UTE-Cones-MT) combined with a modified two-pool rectangular pulse approximation (RP) model has been developed for fast quantitative MT imaging of short T2 tissues using a clinical 3T scanner (18). This UTE-MT modeling can provide a more comprehensive assessment of tissue properties, such as the macromolecular fraction (MMF) (19,20). More importantly, these UTE-MT biomarkers are insensitive to the magic angle effect (19), making them ideal candidates for quantitative evaluation of meniscal degeneration.

In this study, we aimed to evaluate biomarkers derived from 3D UTE-Cones-MT imaging, including the MMF and MTR, in differentiating healthy subjects from patients with mild and advanced OA, and to assess their correlations with the morphological assessment of meniscal degeneration using a modified whole-organ magnetic resonance imaging score (WORMS) (21,22).

Materials and methods

Subjects

A total of 48 human subjects (aged 20-88 years, mean age 55±16 years; 21 males) was recruited from July 2017 to February 2018 for quantitative whole knee MR imaging. Informed consent was obtained from all subjects following guidelines of the University of California San Diego Institutional Review Board. The exclusion criteria included patients with previous knee surgery or traumatic knee injury, knee tumor, infectious lesion, incomplete clinical data, and/or poor image quality (e.g., strong motion artifacts). The definition criteria for OA patients were based on plain radiographs using the Kellgren-Lawrence (KL) OA classification system (Grade 0: no pathological features; Grade 1: doubtful narrowing of joint space and possible osteophytic lipping; Grade 2: definite osteophytes and possible narrowing of joint space; Grade 3: moderate multiple osteophytes, definite narrowing of joint space, some sclerosis, and possible deformity of bony ends; Grade 4: large osteophytes, marked narrowing of joint space, severe sclerosis, and definite deformity of bone ends) (4–7). The definition criteria for healthy subjects were as follows: no history of diagnosed OA and no functional impairment or moderate to severe physical symptoms in the past six months in either knee joint. Of the 48 subjects, 17 were classified as healthy (KL grade 0, 20-49 years; 7 males), 19 were classified as mild OA (KL grade 1 or 2, 37-86 years; 10 males), and 12 were classified as advanced OA (KL grade 3 or 4, 52-88 years; 4 males)

MRI Protocol

Whole knee joint imaging was performed using the 2D sagittal T2-weighted fat-suppressed fast spin echo (T2-FSE) sequence, the 3D UTE with fat suppression (UTE-FS), and the 3D UTE-Cones-MT sequence on a 3T MR750 scanner (GE Healthcare Technologies, Milwaukee, WI). An 8-channel knee coil was used for signal excitation and reception. The fat suppression T2-FSE sequence used the following imaging parameters: TR = 4500 ms, TE = 70.5 ms, field of view = 15×15 cm^2, slice thickness = 3 mm, scan time = 1 min 40

sec, receiver bandwidth = 162 kHz. The 3D UTE-Cones-MT sequence used the following imaging parameters (23): field of view= 15×15×10.8 cm^3, matrix size = 256×256×36, slice thickness = 3.0 mm, voxel size = 0.59 ×0.59×3.0 mm^3, bandwidth = 166 kHz, TR = 100 ms, TE = 32 μs, flip angle (FA) = 7°, number of spokes per MT preparation = 11 (to speed up UTE-Cones-MT data acquisition by 11-fold), three MT powers of 500°, 1000°, and 1500°, and five MT frequency offsets of 2, 5, 10, 20, and 50 kHz, with a total scan time of 14 min 30 sec. The 3D UTE-FS sequence used similar imaging parameters, except a shorter TR of 45 ms, chemical-shift fat saturation, and a scan time of 3 min 40 sec.

Morphological MRI Analysis

Clinical assessment of meniscus and cartilage was performed by two experienced radiologists (22 years of experiences and 16 years of experiences, respectively) evaluating the sagittal fat-suppressed T2-FSE images. Both radiologists were blinded to subject information and quantitative UTE data and performed independent morphological evaluation. In case of disagreement, the two radiologists reached a consensus through consultation. The meniscal WORMS score was graded as follows: 0 = no lesion, 1 = intrasubstance abnormality, 2 = non-displaced tear, 3 = displaced or complex tear without deformity, and 4 = maceration of the meniscus (22). Meniscal score 0 was classified as normal, score 1 as degeneration without tear, and scores 2 through 4 as meniscal tear. The meniscal compartments assessed included the following (4): anterior horn lateral meniscus (AHLAT), anterior horn medial meniscus (AHMED), posterior horn lateral meniscus (PHLAT), and posterior horn medial meniscus (PHMED). The cartilage WORMS score was graded as follows: normal thickness and signal (cartilage WORMS score 0); non-full-thickness cartilage lesions (cartilage WORMS score 1-2); and full-thickness cartilage lesions (cartilage WORMS score 2.5-6) (22). The tibiofemoral compartments were analyzed.

Quantitative MRI Analysis

The elastix motion registration was applied to the 3D UTE-Cones-MT data before quantification (23,24). The whole 3D UTE-Cones-MT data acquisition took about 14.5 min, but each data subset took less than one minute. It is therefore reasonable to consider only inter-scan motion and ignore intra-scan motion. Rigid registration was first carried out to correct for translations and rotations, followed subsequently by non-rigid registration for further fine adjustment (such as scaling and shearing) (23). Each sub-compartment of the meniscus was segmented on three consecutive slices. The MMF and MTR were calculated for medial and lateral menisci following published procedures (18–20). The MMF was calculated by fitting the acquired 15 sets of UTE-Cones-MT data using the modified two-pool MT model (18). The MTR was calculated as the signal difference between the MT data with almost no MT effect(flip angle of 500° and frequency offset of 50 kHz) and the data with maximum MT effect (flip angle of 1500° and frequency offset of 2 kHz) normalized to the signal of the data with almost no MT effect. All segmentation and MT measurements were completed using an in-house developed program in Matlab (Mathworks 2017, Natick, MA). The three continuous midsagittal slices were selected so that the measurements were consistent in the same location across all the knees.

Statistical Analysis

All statistical analyses were completed using SPSS software (Version 23.0, IBM SPSS Statistics, USA). The normality and homogeneity of variance was tested by Shapiro-Wilk test and Levene test, respectively. The continuous variables were compared among groups using one-way ANOVA or Kruskal-Wallis test, while Bonferroni correction was employed for multiple comparisons. The intraclass correlation coefficient (ICC) was used to assess intraobserver variability and reliability. Spearman correlation coefficients of MMF and MTR with meniscal WORMS scores and ages were calculated. The diagnosis efficiency of MMF and MTR was performed by using receiver operating characteristic (ROC) curve and area under the curve (AUC) analyses to differentiate OA patients from healthy volunteers. A *p*-value less than 0.05 indicates statistical significance.

Results

Representative clinical T2-FSE and UTE images as well as maps of MMF and MTR for knee menisci of a normal volunteer, a patient with mild OA and a patient with more advanced OA, respectively, were shown in Figure 1. Menisci show as near-zero signal with the T2-FSE sequence but as a high signal with the UTE sequence, allowing volumetric mapping of MMF and MTR for quantitative assessment of meniscal degeneration. Both MMF and MTR decrease with meniscal degeneration. More details about MMF calculation from two-pool UTE-MT modeling was shown in supplemental Figure 1.

The subject characteristics stratified by three groups of meniscal grades and cartilage scores based on meniscal WORMS assessment were shown as supplemental Table 1.

Decreased MMF and MTR were observed in mild and advanced OA, as shown in Table 1 and Figure 1. The healthy menisci showed the highest MMF and MTR, while the menisci of patients with advanced OA showed the lowest MMF and MTR. Meanwhile, decreased MMF and MTR were observed in menisci with tears (Grade 2-4) or in menisci without tears but degenerated (Grade 1), when compared with normal menisci (Grade 0), as shown in Table 2. Decreased MMF and MTR were also observed in menisci with full-thickness or non-full-thickness cartilage lesions compared with menisci with normal cartilage, as shown in Table 3. Furthermore, the MMF and MTR of AHLAT, MMF of PHLAT, and MTR of PHMED followed normality distribution and homogeneous variance, while the MMF of AHMED and PHMED, and MTR of PHLAT and PHMED did not. The ICC for MMF and MTR measurements were 0.820 (95% CI: 0.721-0.885) and 0.901 (95% CI: 0.838-0.939), respectively.

Significant correlations were observed between the MMF and meniscal WORMS scores, as well as between the MTR and meniscal WORMS scores, with r values of −0.769 (95%CI: −0.695~−0.824, $P<0.01$) and −0.320 (95%CI: −0.168~−0.447, $P<0.01$), respectively, as shown in Figure 2. There was a mild negative correlation between the MMF and age (r=−0.438, 95%CI: −0.317~−0.543, $P<0.01$), as well as between the MTR and age (r=−0.289, 95%CI: −0.146~−0.428, $P<0.01$). Figure 3 shows the ROC curves for the MMF and MTR. The AUC of the MMF and MTR values for differentiating OA patients from healthy volunteers were 0.762 (95%CI: 0.696~0.821) and 0.699 (95%CI: 0.629~0.763),

respectively. With a cut off of MMF≤15.95%, the corresponding sensitivity and specificity were 70.97% and 70.59%, and with a cut off of MTR≤0.56, the corresponding sensitivity and specificity were 84.68% and 50%, respectively. In addition, the posterior horn meniscal MMF and MTR values performs best in differentiating OA patients from healthy volunteers via ROC curve analysis with AUC of 0.835 (95%CI: 0.700~0.926) and 0.883 (95%CI:0.758~0.958), respectively. With a cut off of MMF≤14.86%, the corresponding sensitivity and specificity were 67.74% and 94.12%, and with a cut off of MTR≤0.56, the corresponding sensitivity and specificity were 87.10% and 82.35%, respectively.

Discussion

This is the first study evaluating 3D UTE-Cones-MT imaging of meniscal degeneration and its potential for diagnosis of early OA. Our preliminary results show higher MMF and MTR in healthy menisci and lower MMF and MTR in menisci of patients with mild and advanced OA. At the same time, MMF and MTR are significantly negatively correlated with meniscal WORMS score. A good diagnostic curve was achieved using the MMF and MTR of the four meniscal horns for differentiating OA patients from healthy volunteers, with an AUC of 0.762 and 0.699, respectively. The MMF and MTR of the posterior horn of the medial meniscus further improve diagnosis with an AUC of 0.835 and 0.883, respectively, consistent with the literature which states that meniscal degeneration occurs mostly in this region (25,26). Our preliminary results indicate that the MMF and MTR derived from 3D UTE-Cones-MT imaging are excellent biomarkers for assessing meniscal degeneration and differentiating healthy subjects from mild or advanced OA.

While T1ρ and T2 have been investigated extensively in the evaluation of meniscal degeneration (4–7), the MT technique has received relatively less attention (14). This research mainly focused on measuring MMF through two-pool modeling of 3D UTE-Cones-MT images of healthy and abnormal menisci in vivo (12). MTR values were calculated as a by-product. In MT imaging, the off-resonance saturation pulse partially saturates magnetizations of collagen backbone protons or protons of water bound to collagen, thus indirectly assessing macromolecular content in tissues such as the meniscus and cartilage (12,13). The most common quantitative biomarker is MTR, which represents the percentage of signal reduction due to partial saturation of macromolecules. Most studies suggest that the collagen component is the most important contributor to the MT effect (26–29), but there is an increasing number of studies that associate MTR with glycosaminoglycan concentration and tissue structure (13,30). MTR measurement is influenced by hardware (e.g., field strength) and many other factors such as the MT pulse power and the frequency offset (31). In contrast, hardware and imaging parameters do not affect MMF measurement. Therefore, MMF is believed to be a more robust biomarker than MTR. The preliminary results are encouraging, with excellent separation between normal, mild, and advanced OA groups. MMF and MTR are negatively correlated with meniscal WORMS scores and age. The best correlation is found between meniscal WORMS scores and MMF ($r=-0.769$), whereas weaker correlations are found between age and MMF ($r=-0.438$) and MTR ($r=-0.289$), respectively, indicating that degeneration related composition changes in the meniscus can be effectively detected. Both MMF and MTR measurements showed statistically significant

differences between different levels of knee arthritis groups (Table 1). MMF outperforms MTR and is a more reliable biomarker for knee joint degeneration.

The success of the 3D UTE-Cones-MT imaging and two-pool modeling technique depends on four major factors. First, the 3D UTE-Cones sequence is highly efficient in imaging short T2 tissues such as the meniscus. The Cones trajectory enables fast k-space sampling with a much higher duty cycle than the conventional radial trajectory. The drawback is increased spatial blurring associated with extended spiral sampling, though this is less of a problem for the meniscus as its T2 of ~5 ms is in actuality not extremely short (it is much longer than that of cortical bone, which is on the order of ~0.3 ms (32), thus allowing extended sampling with minimal spatial blurring (33). Second, the 3D multi-spoke UTE-Cones-MT acquisition scheme further improves the efficiency by reducing the total scan time by a factor of Nsp, which is the number of spokes per MT preparation. Third, the modified RP model allows accurate estimation of MMF even with an acceleration factor of Nsp, as demonstrated by Ma et al. (18). Fourth, two-pool MT modeling derived MMF is insensitive to the magic angle effect (19). This is a significant advantage over conventional T2 and T1ρ biomarkers, which may increase by 100-300% when the collagen fibers are reoriented from 0° to 54° relative to the B0 field (9). This magic angle-induced increase may be significantly more than changes induced by degeneration (34). In contrast, the MMF is nearly magic angle-insensitive. A decrease in MMF is likely due to collagen loss or water increase rather than angular orientation. Because of this excellent magic angle insensitivity, the MMF performs much better than the MTR in separating normal menisci from mild or advanced OA.

In addition, the multi-spoke 3D UTE-Cones-MT sequence combined with the two-pool RP modeling allows quantitative assessment of MMF of not only meniscus, but other short T2 tissues such as deep cartilage, tendons, ligaments, and bone. For example, Jerban et al. measured the MMF of cortical bone by using the two-pool 3D UTE-Cones-MT model in an ex vivo study (35). The results showed that the MMF correlated strongly negatively with μCT-based bone porosity and strongly positively with bone mineral density. In this study, decreased MMF and MTR were observed in menisci of mild or advanced OA as compared with menisci of healthy subjects, which was consistent with the loss of macromolecules during the development of OA. Likely, loss of macromolecules may also be observed in other knee joint tissues, including the superficial and deep layers of articular cartilage, ligaments, tendons, and bone. The 3D UTE-Cones-MT imaging and two-pool RP modeling technique can be easily applied to all the knee joint tissues, thus providing a truly “whole-organ” approach for assessment of knee joint degeneration (36), which will be investigated in future studies.

There are several limitations to this study. First, the relatively small sample size of 48 human subjects, especially only 12 subjects with advanced OA, may have limited the statistical power. Second, it is unclear whether the MMF and MTR are correlated with symptoms and function in subjects with knee injury and OA. The knee injury and osteoarthritis outcome score (KOOS) is not available in our study (4), which is a significant limitation. Compared to WORMS which is more subjective, the MMF and MTR may have advantages in a longitudinal study of meniscal degeneration. Third, the ROC curves have relatively low sensitivity and specificity, which may be limited by the small sample size as well as the

lack of a good reference standard in evaluating meniscal degeneration and knee OA. The meniscal WORMS score and the cartilage WORMS score are both subjective and may not provide an accurate assessment of meniscal degeneration. Fourth, age may be a major confounding factor in the quantitative evaluation of meniscal degeneration. The strong correlation between MMF and WORMS together with a much weaker correlation between MMF and age suggests the potential value of MMF in evaluating meniscal degeneration. However, a larger cohort of patients as well as age-matched healthy volunteers will be required for a more systematic evaluation of potential confounders including age, gender, and body mass index (BMI). Lastly, the MMF and MTR were calculated only for the menisci. Quantitative information about other knee joint tissues was not processed in this study.

In conclusion, the multi-spoke 3D UTE-Cones-MT imaging together with two-pool RP modeling of MMF as well as a simple calculation of MTR can be used to evaluate meniscal degeneration in vivo. Decreased meniscal MMF and MTR were observed in mild and advanced OA as compared to healthy ones, showing a negative correlation with the meniscal WORMS score. The 3D UTE-Cones-MT biomarkers can potentially detect compositional changes in the menisci and can be used to differentiate healthy subjects from patients with mild or advanced OA.

Supplementary Material

Refer to Web version on PubMed Central for supplementary material.

Funding and role of the funding source

The authors acknowledge grant support from NIH (R01AR075825, 2R01AR062581, 1R01 AR068987, R21AR075851), VA Clinical Science and Rehabilitation R&D Awards (I01CX001388 and I01RX002604), and GE Healthcare.

References

1. Link TM, Steinbach LS, Ghosh S, Ries M, Lu Y, Lane N, et al. Osteoarthritis: MR imaging findings in different stages of disease and correlation with clinical findings. Radiology 2003; 226(2):373–81. [PubMed: 12563128]
2. Antony B, Driban JB, Price LL, Lo GH, Ward RJ, Nevitt M, et al. The relationship between meniscal pathology and osteoarthritis depends on the type of meniscal damage visible on magnetic resonance images: data from the Osteoarthritis Initiative. Osteoarthritis Cartilage 2017; 25(1):76–84. [PubMed: 27539889]
3. Eijgenraam SM, Bovendeert FAT, Verschueren J, van Tiel J, Bastiaansen-Jenniskens YM, Wesdorp MA, et al. T_2 mapping of the meniscus is a biomarker for early osteoarthritis. Eur Radiol 2019; 29:5664–5672. [PubMed: 30888480]
4. Wang A, Pedoia V, Su F, Abramson E, Kretzschmar M, Nardo L, et al. MR T1ρ and T2 of meniscus after acute anterior cruciate ligament injuries. Osteoarthritis and Cartilage 2016; 24(4):631–9. [PubMed: 26620091]
5. Kajabi AW, Casula V, Nissi MJ, Peuna A, Podlipská J, Lammentausta E, et al. Assessment of meniscus with adiabatic T1ρ and T2ρ relaxation time in asymptomatic subjects and patients with mild osteoarthritis: a feasibility study. Osteoarthritis and Cartilage 2018; 26(4):580–587. [PubMed: 29269326]

6. Zarins ZA, Bolbos RI, Pialat JB, Link TM, Li X, Souza RB, et al. Cartilage and meniscus assessment using T1rho and T2 measurements in healthy subjects and patients with osteoarthritis. Osteoarthritis and Cartilage 2010; 18(11):1408–16. [PubMed: 20696262]
7. Rauscher I, Stahl R, Cheng J, Li X, Huber MB, Luke A, et al. Meniscal Measurements of $T1_{\rho}$ and T2 at MR Imaging in Healthy Subjects and Patients with Osteoarthritis. Radiology 2008; 249(2):591–600. [PubMed: 18936315]
8. Xia Y Magic-Angle Effect in Magnetic Resonance Imaging of Articular Cartilage. Invest Radiol 2000; 35(10):602–621. [PubMed: 11041155]
9. Shao H, Pauli C, Li S, Ma Y, Tadros AS, Kavanaugh A, et al. Magic angle effect plays a major role in both T1rho and T2 relaxation in articular cartilage. Osteoarthritis and Cartilage 2017; 25(12):2022–2030. [PubMed: 28161394]
10. Gray ML, Burstein D, Lesperance LM, Gehrke L. Magnetization transfer in cartilage and its constituent macromolecules. Magn Reson Med 1995; 34(3):319–25. [PubMed: 7500869]
11. Li W, Hong L, Hu L, Magin RL. Magnetization transfer imaging provides a quantitative measure of chondrogenic differentiation and tissue development. Tissue Eng Part C Methods 2010; 16(6):1407–15. [PubMed: 20373975]
12. Zuo H, Yao W, Qu N, Yang S, Wang J, Cui X. Quantitative evaluation in combination with nonquantitative evaluation in early patellar cartilage osteoarthritis at 3.0T. Clin Interv Aging. 2014;16;(9):1133–43.
13. Regatte RR, Akella SV, Reddy R. Depth-dependent proton magnetization transfer in articular cartilage. J Magn Reson Imaging 2005; 22(2):318–23. [PubMed: 16028240]
14. Adler RS, Swanson SD, Doi K, Craig JG, Aisen AM. The effect of magnetization transfer in meniscal fibrocartilage. Magn Reson Med 1996; 35(4):591–5. [PubMed: 8992211]
15. Petersen W, Tillmann B. Collagenous fibril texture of the human knee joint menisci. Anat Embryol (Berl) 1998; 197(4):317–24. [PubMed: 9565324]
16. Du J, Carl M, Diaz E, Takahashi A, Han E, Szeverenyi N, et al. Ultrashort TE T1rho (UTE T1rho) Imaging of the Achilles Tendon and Meniscus. Magn Reson Med 2010 Sep; 64(3):834–42. [PubMed: 20535810]
17. McWalter EJ, Gold GE. UTE T2* mapping detects sub-clinical meniscus degeneration. Osteoarthritis and Cartilage 2012 Jun; 20(6):471–2. [PubMed: 22406647]
18. Ma YJ, Chang EY, Carl M, Du J. Quantitative magnetization transfer ultrashort echo time imaging using a time-efficient 3D multispoke Cones sequence. Magn Reson Med 2018; 79(2):692–700. [PubMed: 28470838]
19. Ma YJ, Shao H, Du J, Chang EY. Ultrashort echo time magnetization transfer (UTE-MT) imaging and modeling: magic angle independent biomarkers of tissue properties. NMR Biomed 2016; 29(11):1546–52. [PubMed: 27599046]
20. Ma YJ, Tadros A, Du J, Chang EY. Quantitative two-dimensional ultrashort echo time magnetization transfer (2D UTE-MT) imaging of cortical bone. Magn Reson Med 2018; 79(4):1941–49. [PubMed: 28776754]
21. Peterfy CG, Guermazi A, Zaim S, Tirman PF, Miaux Y, White D, et al. Whole-Organ Magnetic Resonance Imaging Score (WORMS) of the knee in osteoarthritis. Osteoarthritis and Cartilage 2004; 12(3):177–190. [PubMed: 14972335]
22. Laberge MA, Baum T, Virayavanich W, Nardo L, Nevitt MC, Lynch J, McCulloch CE, Link TM. Obesity increases the prevalence and severity of focal knee abnormalities diagnosed using 3T MRI in middle-aged subjects —data from the Osteoarthritis Initiative. Skeletal Radiol 2012; 41(6): 633–41. [PubMed: 21887596]
23. Wu M, Zhao W, Wan L, Kakos L, Li L, Jerban S, et al. Quantitative three-dimensional ultrashort echo time cones imaging of the knee joint with motion correction. NMR Biomed. 2020 Jan;33(1):e4214. [PubMed: 31713936]
24. Periaswamy S, Farid H. Elastic registration in the presence of intensity variations. IEEE Trans Med Imaging 2003; 22(7):865–74. [PubMed: 12906240]
25. Englund M, Guermazi A, Gale D, Hunter DJ, Aliabadi P, Clancy M, et al. Incidental meniscal findings on knee MRI in middle-aged and elderly persons. New Engl J Med 2008; 359(11):1108–15. [PubMed: 18784100]

26. Kumm J, Roemer FW, Guermazi A, Turkiewicz A, Englund M. Natural History of Intrameniscal Signal Intensity on Knee MR Images: Six Years of Data from the Osteoarthritis Initiative. Radiology 2016; 278(1):164–71. [PubMed: 26172533]
27. Henkelman RM, Stanisz GJ, Graham SJ. Magnetization transfer in MRI: a review. NMR Biomed 2001; 14(2):57–64. [PubMed: 11320533]
28. Kim DK, Ceckler TL, Hascall VC, Calabro A, Balaban RS. Analysis of water-macromolecule proton magnetization transfer in articular cartilage. Magn Reson Med 1993; 29(2):211–5. [PubMed: 8429785]
29. Seo GS, Aoki J, Moriya H, et al. Hyaline cartilage: in vivo and in vitro assessment with magnetization transfer imaging. Radiology 1996; 201(2):525–30. [PubMed: 8888253]
30. Laurent D, Wasvary J, Yin J, Rudin M, Pellas TC, O'Byrne E. Quantitative and qualitative assessment of articular cartilage in the goat knee with magnetization transfer imaging. Magn Reson Imaging 2001; 19(10):1279–86. [PubMed: 11804755]
31. Sinclair CD, Samson RS, Thomas DL, Weiskopf N, Lutti A, Thornton JS, et al. Quantitative magnetization transfer in in vivo healthy human skeletal muscle at 3 T. Magn Reson Med. 2010 Dec; 64(6): 1739–48. [PubMed: 20665899]
32. Du J, Carl M, Bydder M, Takahashi A, Chung CB, Bydder GM. Qualitative and quantitative ultrashort echo time (UTE) imaging of cortical bone. J Magn Reson 2010; 207(2):304–11. [PubMed: 20980179]
33. Wan L, Ma Y, Yang J, Jerban S, Searleman AC, Carl M, et al. Fast quantitative three-dimensional ultrashort echo time (UTE) Cones magnetic resonance imaging of major tissues in the knee joint using extended sprial sampling. NMR Biomed 2020 Jul 15; e4376. [PubMed: 32667115]
34. Mosher TJ, Zhang Z, Reddy R, Boudhar S, Milestone BN, Morrison WB, et al. Knee articular cartilage damage in osteoarthritis: analysis of MR image biomarker reproducibility in ACRIN-PA 4001 multicenter trial. Radiology 2011; 258(3):832–42. [PubMed: 21212364]
35. Jerban S, Ma Y, Wong JH, Nazaran A, Searleman A, Wan L, et al. Ultrashort echo time magnetic resonance imaging (UTE-MRI) of cortical bone correlates well with histomorphometric assessment of bone microstructure. Bone 2019 Jun; 123:8–17. [PubMed: 30877070]
36. Loeser RF, Goldring SR, Scanzello CR, Goldring MB. Osteoarthritis: A disease of the joint as an organ. Arthritis and rheumatism 2012; 64(6):1697–707. [PubMed: 22392533]

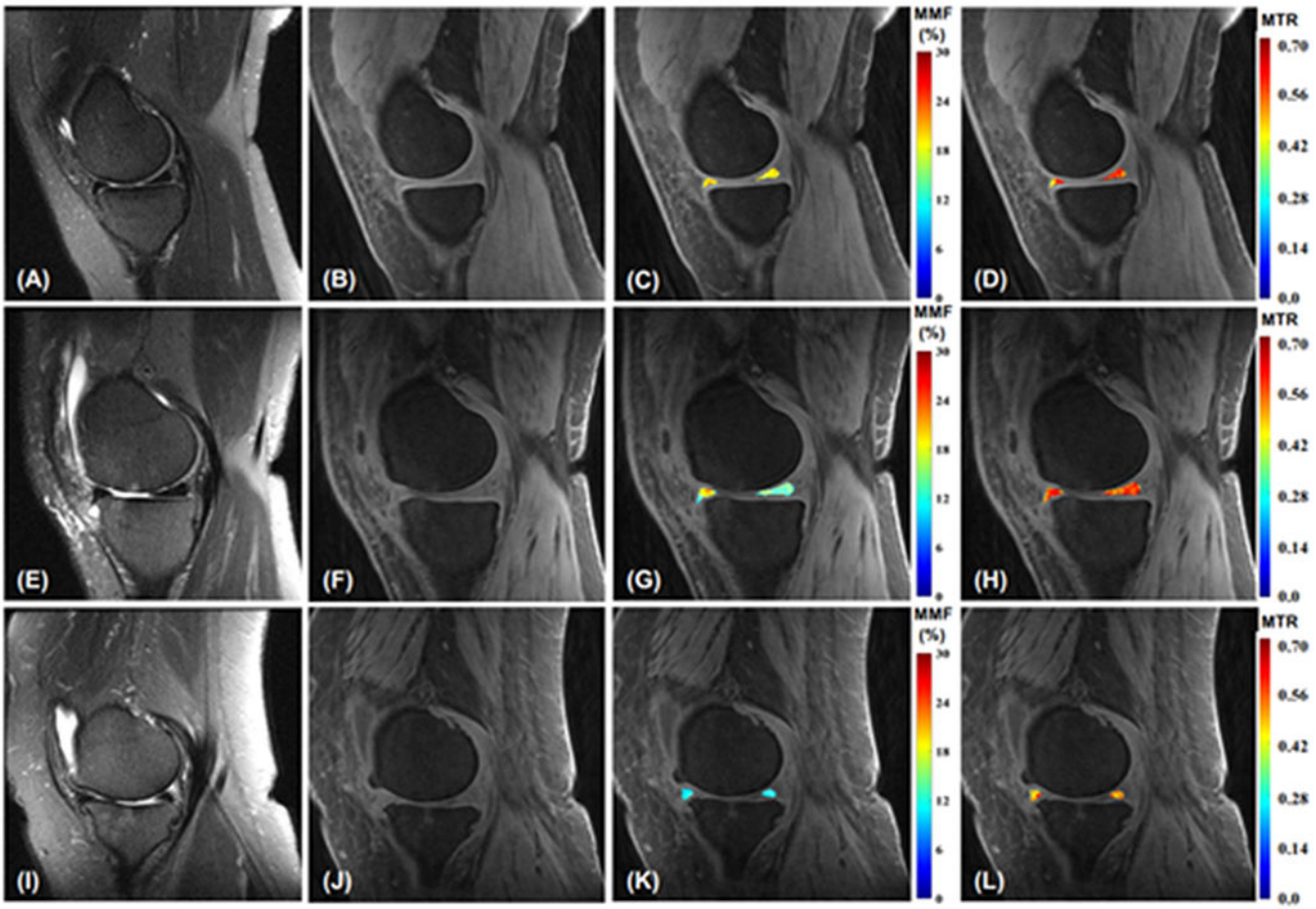

Figure 1.

A 23-year-old female healthy volunteer imaged with T2 fast spin echo (T2-FSE) (A) and ultrashort echo time (UTE) (B) sequences, as well as the corresponding macromolecular fraction (MMF) (C) and magnetization transfer ratio (MTR) (D) maps, a 58-year-old male with mild osteoarthritis (OA), imaged with T2-FSE (E) and UTE (F) sequences and corresponding MMF (G) and MTR (H) maps, and a 68-year-old female with advanced OA imaged with T2-FSE (I) and UTE (J) sequences as well as the corresponding MMF (K) and MTR (L) maps. Decreased MMF and MTR were observed in abnormal menisci.

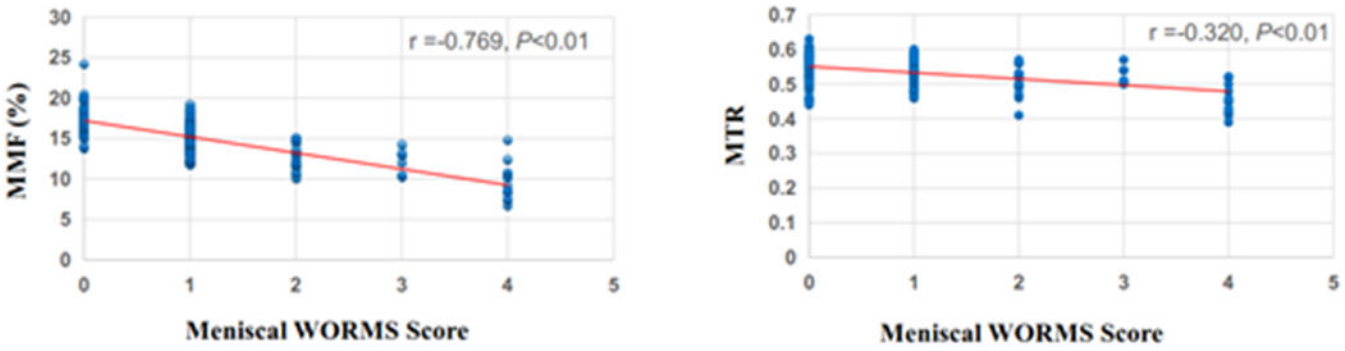

Figure 2.

Scatter diagram of the correlations of macromolecular fraction (MMF) with meniscal WORMS scores (a) and magnetization transfer ratio (MTR) with meniscal WORMS score (b). The mean MMF and MTR decreased with WORMS scores of meniscus increasing.

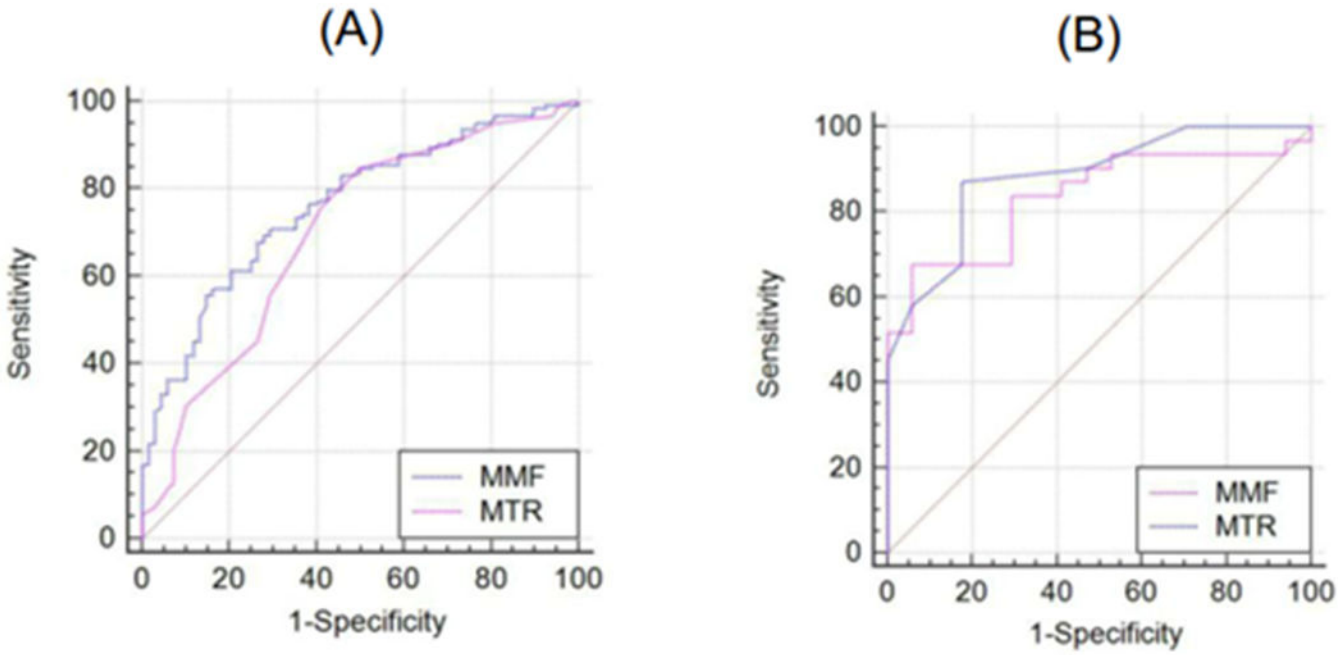

Figure 3.

(A)The area under the curve (AUC) values of the whole meniscal macromolecular fraction (MMF) and magnetization transfer ratio (MTR) values for differentiating osteoarthritis (OA) patients from healthy volunteers via receiver operating characteristic (ROC) curve analysis were 0.762 and 0.699, respectively, with no significant difference between them (P>0.05). (B)The area under the curve (AUC) values of the posterior horn medial macromolecular fraction (MMF) and magnetization transfer ratio (MTR) values for differentiating osteoarthritis (OA) patients from healthy volunteers via receiver operating characteristic (ROC) curve analysis were 0.835 and 0.883, respectively, with no significant difference between them (P>0.05).

Table 1:

The median and interquartile range values for 3D UTE-quantitative values of MMF and MTR in healthy subjects and patients with mild or advanced OA.

Meniscus	Healthy (Group A)	Mild OA (Group B)	Advanced OA (Group C)	*P*-value	*Adjusted P*-value A vs B	*Adjusted P*-value A vs C	*Adjusted P*-value B vs C
MMF (%)							
AHLAT	15.84(14.72, 16.97)	14.30(12.73,15.37)	13.24(11.99,14.35)	0.008*	0.066	0.010*	1.000
PHLAT	17.29(16.03,18.55)	15.40(14.81,16.62)	14.00(11.02,17.06)	0.010*	0.146	0.009*	0.640
AHMED	17.78(17.26,18.31)	16.28(15.05,17.31)	15.30(13.17,16.92)	0.002*	0.012*	0.004*	1.000
PHMED	16.35(15.83,16.87)	14.84(12.36,15.70)	12.82(9.44,14.45)	0.000*	0.016*	0.000*	0.367
MTR							
AHLAT	0.54(0.52,0.57)	0.53(0.51,0.55)	0.49(0.48,0.53)	0.028*	0.276	0.026*	0.740
PHLAT	0.57(0.55,0.58)	0.55(0.54,0.57)	0.52(0.47,0.56)	0.034*	0.301	0.032*	0.782
AHMED	0.53(0.51,0.54)	0.51(0.49,0.54)	0.53(0.51,0.56)	0.228	–	–	–
PHMED	0.58(0.57,0.58)	0.54(0.53,0.56)	0.53(0.48,0.56)	0.000*	0.001*	0.000*	0.950

Note. AHLAT, anterior horn lateral; PHLAT, posterior horn lateral; AHMED, anterior horn medial; PHMED, posterior horn medial

*, $P<0.05$.

Table 2:

The median and interquartile range values for 3D UTE-quantitative values of MMF and MTR in subjects with normal meniscus (Grade 0), no meniscal tear (Grade 1), and meniscal tear (Grade 2-4)

Meniscus	Normal (Grade 0)	Degeneration without tear (Grade 1)	Meniscal Tear (Grade 2-4)	*P*-value	*Adjusted P*-value (Grade 0 vs 1)	*Adjusted P*-value (Grade 0 vs 2-4)	*Adjusted P*-value (Grade 1 vs 2-4)
MMF (%)							
AHLAT	17.04(15.96,18.04)	13.94(13.10,14.88)	11.76(9.66,13.03)	0.000 *	0.000 *	0.000 *	0.054
PHLAT	18.19(16.12,18.91)	15.43(14.54,17.22)	11.02(9.03,12.37)	0.000 *	0.051	0.000 *	0.005 *
AHMED	17.54(16.62,18.28)	14.77(12.72,15.93)	11.92(10.65,13.19)	0.000 *	0.000 *	0.024 *	1.000
PHMED	16.81(16.31,17.30)	15.63(14.76,16.20)	11.78(10.36,14.00)	0.000 *	0.154	0.000 *	0.000 *
MTR							
AHLAT	0.56(0.55,0.57)	0.53(0.48,0.54)	0.49(0.43,0.52)	0.001 *	0.023 *	0.001 *	0.244
PHLAT	0.58(0.55,0.59)	0.55(0.53,0.57)	0.50(0.43,0.52)	0.000 *	0.223	0.000 *	0.015 *
AHMED	0.52(0.50,0.55)	0.52(0.50,0.56)	0.50(0.47,0.53)	0.794			
PHMED	0.57(0.56,0.58)	0.56(0.55,0.58)	0.52(0.49,0.54)	0.000 *	1.000	0.001 *	0.001 *

Note. AHLAT, anterior horn lateral; PHLAT, posterior horn lateral; AHMED, anterior horn medial; PHMED, posterior horn medial

*, $P<0.05$.

Table 3:

The median and interquartile range values for 3D UTE-quantitative values of MMF and MTR in different cartilage scales

Meniscus	Normal cartilage (WORMS 0)	Non-full-thickness lesions (WORMS 1-2)	full-thickness lesions (WORMS≥2)	*P*-value	*Adjusted P*-value WORMS 0 vs 1-2	*Adjusted P*-value WORMS 0 vs ≥2	*Adjusted P*-value WORMS 1-2 vs ≥2
MMF (%)							
AHLAT	15.94(13.78,17.09)	14.51(12.58,14.95)	13.40(11.51,14.45)	0.006*	0.064	0.007*	1.000
PHLAT	17.97(15.20,18.96)	15.29(14.57,16.47)	14.27(12.75,17.10)	0.006*	0.060	0.008*	1.000
AHMED	17.70(16.96,18.48)	16.67(15.93,17.91)	14.85(13.12,16.85)	0.002*	0.001*	0.214	0.215
PHMED	16.40(15.49,17.12)	14.76(13.45,15.78)	11.39(9.71,14.85)	0.000*	0.075	0.000*	0.114
MTR							
AHLAT	0.56(0.53,0.57)	0.52(0.48,0.54)	0.51(0.48,0.55)	0.017*	0.103	0.022*	1.000
PHLAT	0.58(0.55,0.59)	0.55(0.51,0.56)	0.53(0.48,0.59)	0.023*	0.032*	0.112	1.000
AHMED	0.52(0.50,0.56)	0.52(0.49,0.54)	0.52(0.50,0.55)	0.951			
PHMED	0.58(0.57,0.59)	0.55(0.53,0.56)	0.52(0.47,0.56)	0.000	0.018*	0.000*	0.245

Note. AHLAT, anterior horn lateral; PHLAT, posterior horn lateral; AHMED, anterior horn medial; PHMED, posterior horn medial

*, $P<0.05$.